Polymer Chemistry

RSC Publishing

PAPER

View Article Online
View Journal | View Issue

Cite this: *Polym. Chem.*, 2013, **4**, 3333

Synthesis, photophysical and photovoltaic properties of a new class of two-dimensional conjugated polymers containing donor–acceptor chromophores as pendant groups†

Yu-Ying Lai, Yen-Ju Cheng,* Chiu-Hsiang Chen, Sheng-Wen Cheng, Fong-Yi Cao and Chain-Shu Hsu*

Received 31st January 2013
Accepted 13th March 2013

DOI: 10.1039/c3py00168g

www.rsc.org/polymers

A new design for constructing two-dimensional conjugated copolymers with the D_1–A(D_2) repeating pattern (A: acceptor, D_1: donor 1, D_2: donor 2; molecules enclosed in parentheses are pendant groups.), is proposed. D_1 and A are employed to construct the linear main-conjugated polymer chain and D_2 is situated at the conjugated side chains connected to A. We designed and synthesized a series of D_1–A(D_2)-type copolymers, in which D_1 = diindeno[1,2-*b*:2′,1′-*d*]-thiophene (**DIDT**) or fluorene (**F**), A(D_2) = bis-[4-(dioctylamino)-phenyl] quinoxaline (**DOAQX**) or bis-[4-(dioctylamino)-phenyl] thieno[3,4-*b*]-pyrazine (**DOATP**), and D_2 = *N*,*N*-dioctylanilines. The resultant copolymers, **PDIDTDOAQX**, **PFDOAQX**, **PDIDTDOATP** and **PFDOATP**, possess at least two strong ICT absorptions, thus resulting in better light harvesting. Their optical and electronic properties were thoroughly investigated experimentally and computationally. Bulk heterojunction photovoltaic cells on the basis of ITO/PEDOT:PSS/polymer:$PC_{71}BM$/Ca/Al configuration were fabricated and characterized. The photovoltaic performances of the devices incorporating these polymers follow the sequence: **PDIDTDOAQX** > **PFDOAQX** > **PDIDTDOATP** > **PFDOATP**, which is in good agreement with the magnitude of their hole-mobilities.

Introduction

Harvesting energy directly from sunlight using photovoltaic technology is considered one of the most promising approaches to address the growing global energy needs. Over the past few years, tremendous scientific effort has been made on organic photovoltaics (OPVs) to accomplish low-cost, lightweight, large-area, and flexible photovoltaic devices.[1] The development of novel conjugated polymers has been demonstrated to be effective in improving the efficiency of OPV cells. To date, there are several design strategies for preparing the conjugated polymers which are classified into (a) D-based polymers,[1e,2,3d] (b) D–A alternating copolymers,[3] (c) D–A random copolymers,[4] (d) D_1(D_2) copolymers,[5] and (e) D_1–D_2(A) copolymers[6] (D: donor, A: acceptor, D_1: donor 1, D_2: donor 2). Parentheses are used to indicate that the enclosed molecules are the pendant groups in the polymer chains. As illustrated in Fig. 1, D-based, D–A alternating, and D–A random polymers belong to one-dimensional conjugated polymers and D_1(D_2) and D_1–D_2(A) polymers are categorized into two-dimensional conjugated polymers. The concept of utilizing two-dimensional architecture can in principle broaden or intensify the absorption of the corresponding polymers. On the other hand, the donor–acceptor strategy has been established to be one of the most useful ways in preparing low band gap (LBG) polymers because of the efficient photo-induced intramolecular charge transfer (ICT) from the donor to the acceptor. Their optical properties can thus be fine-tuned by adjusting the donating ability of the donor and/or the withdrawing strength of the acceptor. Consequently, two-dimensional-polymer construction in association with the D–A tactic, such as D_1–D_2(A), continues to receive attention.

Herein, we propose a new type of two-dimensional conjugated copolymer with the D_1–A(D_2) repeating pattern, where D_1 and A are used to construct the linear main-conjugated system and D_2 is situated at the conjugated side chains connected to A (Fig. 2). Unlike the D_1–D_2(A) system, exchanging the position of D_2 with A can not only preserve the ICT from D_2 to A, but can further enhance the ICT from D_1 to A, resulting in better light harvesting. Based on this viewpoint, a series of D_1–A(D_2)-type copolymers were designed and synthesized, where D_1 = diindeno[1,2-*b*:2′,1′-*d*]-thiophene (**DIDT**)[3c,7] or fluorene (**F**), A(D_2) = bis-[4-(dioctylamino)-phenyl] quinoxaline (**DOAQX**) or bis-[4-(dioctylamino)-phenyl] thieno[3,4-*b*]pyrazine (**DOATP**), and D_2 = *N*,*N*-dioctylanilines (Fig. 2). Their thermal, optical, and electrochemical properties have been characterized and

Department of Applied Chemistry, National Chiao Tung University, 1001 Ta Hseuh Road, Hsin-Chu, 30010 Taiwan. E-mail: yjcheng@mail.nctu.edu.tw; cshsu@mail.nctu.edu.tw

† Electronic supplementary information (ESI) available. See DOI: 10.1039/c3py00168g

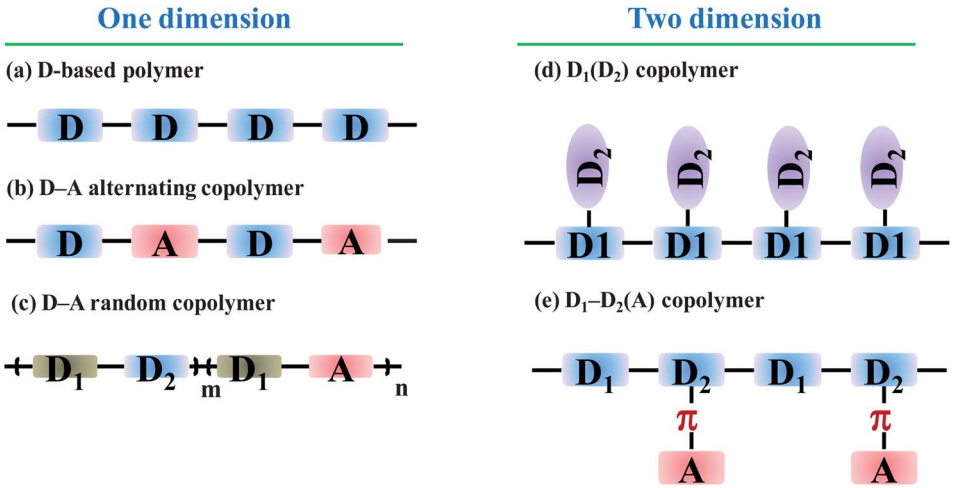

Fig. 1 Molecular architecture for constructing conjugated polymers.

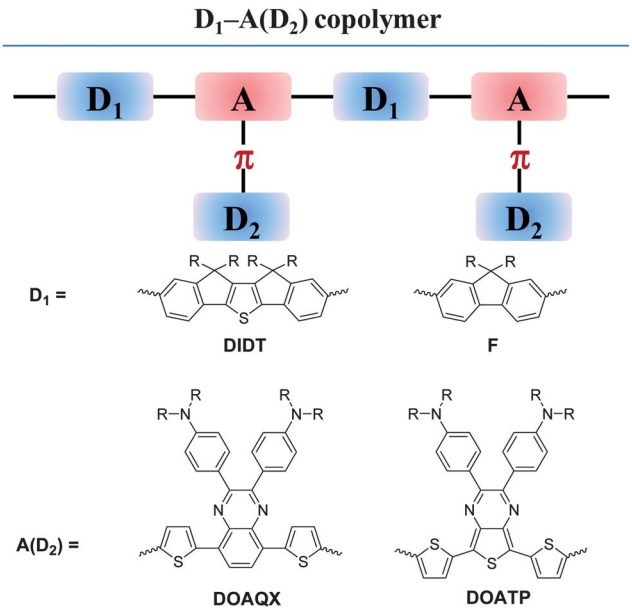

Fig. 2 D_1–$A(D_2)$-type two-dimensional copolymers where D_1 = diindeno[1,2-*b*:2′,1′-*d*]-thiophene (**DIDT**) or fluorene (**F**), $A(D_2)$ = bis-[4-(dioctylamino)-phenyl] quinoxaline (**DOAQX**) or bis-[4-(dioctylamino)-phenyl] thieno[3,4-*b*]pyrazine (**DOATP**), and D_2 = *N*,*N*-dioctylanilines.

theoretical calculations were performed. Preliminary tests of the photovoltaic performance based on these polymers were carried out and investigated.

Experimental

General remarks

All chemicals were purchased from commercial sources and used as received unless otherwise specified. NMR measurements are reported for Varian Unity-300 spectrometers (^{1}H, 300 MHz; ^{13}C, 75 MHZ). Chemical shifts (δ values) are reported in ppm with respect to Me_4Si (δ = 0 ppm) for ^{13}C and ^{1}H NMR. Coupling constants (J) are given in Hz. ^{13}C NMR was proton broad-band-decoupled. Multiplicities of peaks are denoted by the following abbreviations: s, singlet; d, doublet; t, triplet; m, multiplet; br, broad. The molecular weight of polymers was determined by gel permeation chromatography on a Viscotek VE2001GPC instrument. Polystyrene was used as the internal standard and THF is the eluent. Thermogravimetric analyses (TGA) were recorded on a PerkinElmer Pyris analyzer under nitrogen atmosphere at a heating rate of 10 °C min^{-1}. Absorption spectra were collected on a HP8453 UV-Vis spectrophotometer. Electrochemical cyclic voltammetry (CV) was conducted on a Bioanalytical Systems Inc. analyzer. A carbon glass coated with a thin polymer film was used as the working electrode and Ag/AgCl as the reference electrode, while 0.1 M tetrabutylammonium hexafluorophosphate in acetonitrile was the electrolyte. CV curves were calibrated using ferrocene as the standard, whose oxidation potential is set at −4.8 eV with respect to zero vacuum level. The HOMO energy levels were obtained from the equation HOMO = $-(E_{ox}^{onset} - E_{(ferrocene)}^{onset} + 4.8)$ eV. The LUMO levels were obtained from the equation LUMO = $-(E_{red}^{onset} - E_{(ferrocene)}^{onset} + 4.8)$ eV.

Fabrication and characterization of BHJ devices

An indium tin oxide (ITO)-coated glass substrate was ultrasonically cleaned sequentially by detergent, water, acetone and isopropyl alcohol. It was then covered by a 30 nm thick layer of PEDOT:PSS (Clevios P provided by H. C. Stark) by spin-coating, thermally annealed in air at 200 °C for 10 min, and cooled down to room temperature. **PDIDTDOAQX**, **PFDOAQX**, **PDIDTDOATP** and **PFDOATP** were dissolved in *o*-dichlorobenzene (ODCB) (0.5–1.0 wt%), respectively and mixed with $PC_{71}BM$ (purchased from Nano-C). The individual solutions were heated at 70 °C for 1 hour, stirred overnight at room temperature, and filtered through a 0.45 μm filter. The filtrates were then spin-coated on top of the PEDOT:PSS layer at various spin-coating speeds in a glove box in order to tune their film thickness. Subsequent to drying, they were thermally annealed for 15 min. The spin-coating speeds for polymer/$PC_{71}BM$ are described as follows:

PDIDTDOAQX/$PC_{71}BM$ (1000 rpm), **PFDOAQX**/$PC_{71}BM$ (1400 rpm), **PDIDTDOATP**/$PC_{71}BM$ (1400 rpm), and **PFDOATP**/$PC_{71}BM$ (1400 rpm). The top electrode was then prepared by sequential evaporation of calcium (35 nm thick) and aluminum (100 nm thick) through a shadow mask under high vacuum ($<10^{-6}$ torr). All devices contained an active area of 0.04 cm^2 and the photovoltaic parameters were measured under air atmosphere.

Electrical characterization under illumination

The devices were characterized under 100 mW cm^{-2} AM1.5 simulated light (Yamashita Denso solar simulator). Current–voltage (J–V) characteristics of the devices were obtained using a Keithley 2400 SMU. Solar illumination conforming to the JIS Class AAA was provided by a SAN-EI 300W solar simulator equipped with an AM1.5G filter. The light intensity was calibrated with a Hamamatsu S1336-5BK silicon photodiode. The performances are the average of the 4 pixels of each device.

Hole-only devices

In order to investigate the respective hole mobilities of the different polymer films, unipolar devices have been prepared following the same procedure except that the active layer is made of pure polymer and the Ca/Al cathode is replaced by evaporated gold (40 nm). The hole mobilities were calculated according to the space charge limited current theory (SCLC). The J–V curves were fitted according to the following equation:

$$J = \frac{9}{8}\varepsilon\mu\frac{V^2}{L^3}$$

where ε is the dielectric permittivity of the polymer, μ is the hole mobility and L is the film thickness (distance between the two electrodes).

Synthesis of 1,2-bis(4-dioctylaminophenyl)ethane-1,2-dione (4)

To a solution of **2** (31.4 g, 79.2 mmol) in dry THF (125 mL) under nitrogen was added a hexane solution of *n*-BuLi (2.5 M, 65.0 mmol) dropwise at −78 °C. The mixture was stirred at this temperature for 30 min and **3** (5.0 g, 35.2 mmol) was then introduced in one portion. After stirring at −78 °C for 2 h, it was gradually warmed up to room temperature, quenched with 10% HCl solution (100 mL), and extracted with ethyl acetate (400 mL × 3). The collected organic layer was washed with water (200 mL), dried over $MgSO_4$, and evaporated under reduced pressure. The residue was then purified by column chromatography on silica gel (hexane–ethyl acetate, v/v, 50/1) to give a deep yellow oil **4** (17.2 g, 71%): ^{1}H NMR ($CDCl_3$, 300 MHz): 0.88 (t, J = 6.5 Hz, 12H), 1.16–1.42 (m, 40H), 1.50–1.70 (m, 8H), 3.31 (t, J = 7.7 Hz, 8H), 6.57 (d, J = 9.0 Hz, 4H), 7.82 (d, J = 9.0 Hz, 4H); ^{13}C NMR ($CDCl_3$, 75 MHz): 14.1, 22.6, 27.0, 27.1, 29.2, 29.4, 31.8, 51.1, 110.5, 120.9, 132.4, 152.4, 193.7; MS (EI, $M^{+\cdot}$, $C_{46}H_{76}N_2O_2$): calcd, 688.59; found, 689.

Synthesis of 3,6-bis(5-bromothiophen-2-yl)benzene-1,2-diamine (8)

To a solution of **7** (2.0 g, 4.36 mmol) in acetic acid (100 mL) was added zinc dust (5.82 g, 89.0 mmol) in one portion. The reaction mixture was refluxed for 30 min, cooled to room temperature, and filtered. The resulting solid was collected, dissolved in ether (70 mL), and washed with 5% $NaOH_{(aq)}$. After removal of the solvent under reduced pressure, the residue was purified by column chromatography on silica gel (hexane–ethyl acetate, v/v, 10/1) and recrystallized from methanol to give a white powder **8** (0.77 g, 41%): ^{1}H NMR ($CDCl_3$, 300 MHz): 3.83 (br, 4H), 6.79 (s, 2H), 6.92 (d, J = 3.8 Hz, 2H), 7.09 (d, J = 3.8 Hz, 2H); ^{13}C NMR ($CDCl_3$, 75 MHz): 112.1, 120.6, 121.2, 126.6, 130.4, 133.1, 142.5; MS (EI, $M^{+\cdot}$, $C_{14}H_{10}Br_2N_2S_2$): calcd, 429.86; found, 430.

Synthesis of 2,3-bis(4-dioctylaminophenyl)-5,8-bis(5-bromothiophen-2-yl)quinoxaline (9)

8 (0.70 g, 1.62 mmol), **4** (1.68 g, 2.44 mmol), and acetic acid (85 mL) were mixed together and heated at reflux for 3 h. After removal of acetic acid under reduced pressure, the residue was purified by column chromatography on silica gel (hexane–ethyl acetate, v/v, 250/1) to give a red oil **9** (1.19 g, 68%): ^{1}H NMR ($CDCl_3$, 300 MHz): 0.89 (t, J = 7.5 Hz, 12H), 1.20–1.40 (m, 40H), 1.56–1.65 (m, 8H), 3.31 (t, J = 7.5 Hz, 8H), 6.64 (d, J = 8.4 Hz, 4H), 7.10 (d, J = 4.2 Hz, 2H), 7.52 (d, J = 4.2 Hz, 2H), 7.74 (d, J = 8.4 Hz, 4H), 7.91 (s, 2H); ^{13}C NMR ($CDCl_3$, 75 MHz): 14.1, 22.7, 27.2, 27.3, 29.4, 29.5, 31.8, 51.0, 110.8, 116.4, 124.4, 125.0, 125.4, 128.9, 130.0, 131.8, 136.1, 140.3, 148.9, 152.3; MS (FAB, $(M + H)^+$, $C_{60}H_{83}Br_2N_4S_2$): calcd, 1083.44; found, 1084. Anal. calcd for $C_{60}H_{82}Br_2N_4S_2$: C, 66.53; H, 7.63; N, 5.17; found: C, 66.94; H, 7.83; N, 4.97%.

Synthesis of 2,3-bis(4-dioctylaminophenyl)-5,7-bis(5-bromothiophen-2-yl)thieno[3,4-*b*]pyrazine (14)

13 (0.60 g, 1.38 mmol), **4** (1.04 g, 1.51 mmol), and acetic acid (32 mL) were mixed together and heated at 60 °C for 5 h. After removal of acetic acid under reduced pressure, the residue was purified by column chromatography on silica gel (hexane–ethyl acetate, v/v, 250/1) to give a red solid **14** (0.82 g, 55%): ^{1}H NMR ($CDCl_3$, 300 MHz): 0.89 (t, J = 6.9 Hz, 12H), 1.20–1.40 (m, 40H), 1.50–1.70 (m, 8H), 3.30 (t, J = 7.5 Hz, 8H), 6.60 (d, J = 8.9 Hz, 4H), 7.02 (d, J = 4.1 Hz, 2H), 7.24 (d, J = 4.1 Hz, 2H), 7.60 (d, J = 8.9 Hz, 4H); ^{13}C NMR ($CDCl_3$, 75 MHz): 14.1, 22.7, 27.2, 27.3, 29.3, 29.5, 31.9, 51.1, 110.7, 113.6, 122.1, 123.0, 125.8, 129.6, 131.5, 136.7, 137.7, 149.1, 153.6; MS (FAB, $(M + H)^+$, $C_{58}H_{81}Br_2N_4S_3$): calcd, 1089.40; found, 1090. Anal. calcd for $C_{58}H_{80}Br_2N_4S_3$: C, 63.95; H, 7.40; N, 5.14; found: C, 64.04; H, 7.63; N, 4.93%.

Synthesis of PDIDTDOAQX

A mixture of **9** (410 mg, 0.38 mmol), 2,8-bis(4,4,5,5-tetramethyl-[1,3,2]dioxaborolan-2-yl)-10,10,11,11-tetraoctyl-diindeno[1,2-*b*:2′1′-*d*]thiophene (364 mg, 0.38 mmol), $Pd(PPh_3)_4$ (8.7 mg, 0.0076 mmol), K_2CO_3 (395 mg, 2.86 mmol), Aliquant 336 (65 mg, 0.16 mmol), degassed toluene (20 mL), and degassed H_2O (4 mL) was heated to 90 °C under nitrogen atmosphere for 72 h. It was then added to methanol dropwise. The precipitate was collected by filtration and washed by Soxhlet extraction with methanol and acetone sequentially for one week. The crude polymer was dissolved in hot THF and the residual Pd catalyst

in the THF solution was removed by Pd-thiol gel (Silicycle Inc.). After filtration and removal of the solvent, the polymer was re-dissolved in THF again and reprecipitated by methanol. The resultant polymer was collected by filtration and dried under vacuum for 1 day to give a black solid (490 mg, 79%, M_n = 39 000, PDI = 2.00): ^{1}H NMR ($CDCl_3$, 300 MHz): 0.60–1.80 (m, 120H), 2.00–2.25 (m, 8H), 3.20–3.60 (m, 8H), 6.60–6.80 (m, 4H), 7.30–8.10 (m, 16H).

Synthesis of PFDOAQX

A mixture of **9** (280 mg, 0.26 mmol), 2,7-bis(4,4,5,5-tetramethyl-[1,3,2]dioxaborolan-2-yl)-9,9-dioctylfluorene (166 mg, 0.26 mmol), $Pd(PPh_3)_4$ (6.0 mg, 0.005 mmol), K_2CO_3 (270 mg, 1.95 mmol), Aliquant 336 (37 mg, 0.09 mmol), degassed toluene (15 mL), and degassed H_2O (3 mL) was heated to 90 °C under nitrogen atmosphere for 72 h. It was then added to methanol dropwise. The precipitate was collected by filtration and washed by Soxhlet extraction with methanol and acetone sequentially for one week. The crude polymer was dissolved in hot THF and the residual Pd catalyst in the THF solution was removed by Pd-thiol gel (Silicycle Inc.). After filtration and removal of the solvent, the polymer was re-dissolved in THF again and reprecipitated by methanol. The resultant polymer was collected by filtration and dried under vacuum for 1 day to give a dark red solid (250 mg, 73%, M_n = 22 000, PDI = 1.23): ^{1}H NMR ($CDCl_3$, 300 MHz): 0.60–1.80 (m, 90H), 2.00–2.25 (m, 4H), 3.30–3.50 (m, 8H), 6.60–6.80 (m, 4H), 7.40–7.60 (m, 2H), 7.70–8.10 (m, 14H).

Synthesis of PDIDTDOATP

A mixture of **14** (400 mg, 0.37 mmol), 2,8-bis(4,4,5,5-tetramethyl-[1,3,2]dioxaborolan-2-yl)-10,10,11,11-tetraoctyl-diindeno-[1,2-*b*:2′1′-*d*]thiophene (353 mg, 0.37 mmol), $Pd(PPh_3)_4$ (8.5 mg, 0.007 mmol), K_2CO_3 (383 mg, 2.77 mmol), Aliquant 336 (63 mg, 0.16 mmol), degassed toluene (20 mL), and degassed H_2O

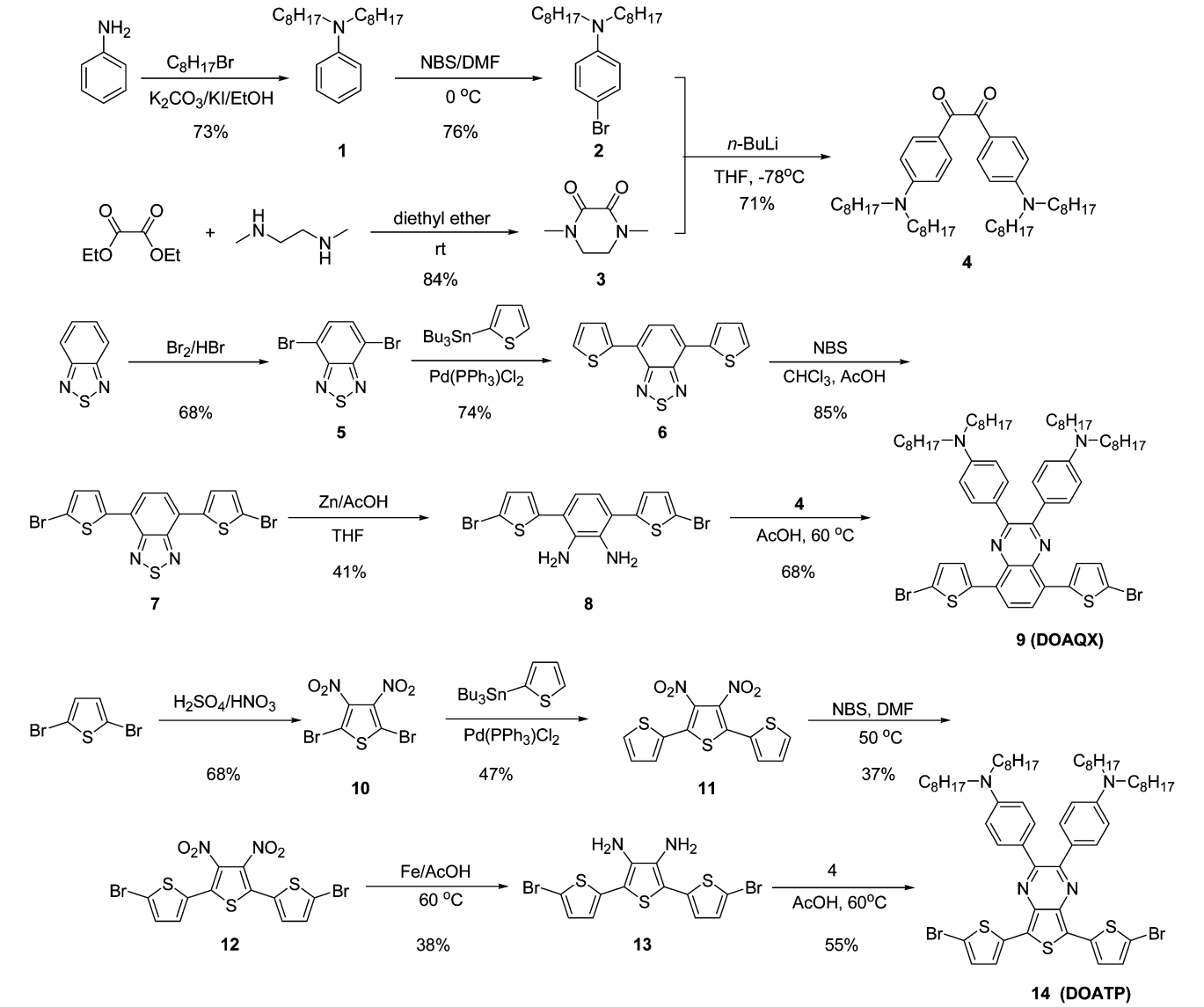

Scheme 1 Synthesis of **DOAQX** and **DOATP**.

(4 mL) was heated to 90 °C under nitrogen atmosphere for 72 h. It was then added to methanol dropwise. The precipitate was collected by filtration and washed by Soxhlet extraction with methanol and acetone sequentially for one week. The crude polymer was dissolved in hot THF and the residual Pd catalyst in the THF solution was removed by Pd-thiol gel (Silicycle Inc.). After filtration and removal of the solvent, the polymer was re-dissolved in THF again and reprecipitated by methanol. The resultant polymer was collected by filtration and dried under vacuum for 1 day to give a black solid (213 mg, 35%, M_n = 12 000, PDI = 1.17): ^{1}H NMR ($CDCl_3$, 300 MHz): 0.60–1.50 (m, 112H), 1.50–1.75 (m, 8H), 1.90–2.20 (m, 8H), 3.20–3.40 (m, 8H), 6.55–6.70 (m, 4H), 7.30–7.45 (m, 4H), 7.50–7.60 (m, 2H), 7.60–7.80 (m, 8H).

Synthesis of PFDOATP

A mixture of **14** (270 mg, 0.25 mmol), 2,7-bis(4,4,5,5-tetramethyl-[1,3,2]dioxaborolan-2-yl)-9,9-dioctylfluorene (159 mg, 0.25 mmol), $Pd(PPh_3)_4$ (5.7 mg, 0.005 mmol), K_2CO_3 (259 mg, 1.87 mmol), Aliquant 336 (43 mg, 0.11 mmol), degassed toluene (14 mL), and degassed H_2O (3 mL) was heated to 90 °C under nitrogen atmosphere for 72 h. It was then added to methanol dropwise. The precipitate was collected by filtration and washed by Soxhlet extraction with methanol and acetone sequentially for one week. The crude polymer was dissolved in hot THF and the residual Pd catalyst in the THF solution was removed by Pd-thiol gel (Silicycle Inc.). After filtration and removal of the solvent, the polymer was re-dissolved in THF again and reprecipitated by methanol. The resultant polymer was collected by filtration and dried under vacuum for 1 day to give a dark red solid (132 mg, 40%, M_n = 12 000, PDI = 1.17): ^{1}H NMR ($CDCl_3$, 300 MHz): 0.60–1.70 (m, 90H), 1.90–2.20 (m, 4H), 3.20–3.40 (m, 8H), 6.55–6.70 (m, 4H), 7.40–7.45 (m, 2H), 7.50–7.80 (m, 12H).

Results and discussion

Synthesis

Synthesis of **DOAQX** and **DOATP** moieties is depicted in Scheme 1. Aniline was treated with an excess amount of *n*-octylbromine in the presence of potassium carbonate and potassium iodide in ethanol to give **1** in 73% yield. Bromination of **1** occurred selectively at the *para* position by *N*-bromosuccinimide (NBS) to furnish compound **2**. Amidation of diethyl oxalate in anhydrous diethylether yielded compound **3**. The key intermediate diketone **4** with two *N*,*N*-dioctylaniline groups was obtained in 71% yield by treatment of the lithiumated compound **2** with compound **3** in THF. Bromination of benzothiadiazole with Br_2/HBr regio-selectively occurred at the 4,7 positions to form compound **5** in 68% yield. Compound **5** was then reacted with tributyl(thiophen-2-yl)stannane in the presence of catalytic amounts of $Pd(PPh_3)_2Cl_2$ to give compound **6**. Compound **7** was synthesized by bromination of compound **6** with NBS, followed by zinc-promoted reduction to form diamine **8**. The formation of quinoxaline dithiophene **9** (**DOAQX**) was achieved by double condensation of **8** with **4**. The other monomer thieno[3,4-*b*]-pyrazine dithiophene **14** (**DOATP**) was synthesized through analogous steps to **9**, which are illustrated in Scheme 1. The A(D_2) units, **DOAQX** and **DOATP** were then polymerized respectively with D_1 units, 2,8-diboronic ester-**DIDT**[3c] and 2,7-diboronic ester-fluorene *via* Suzuki cross-coupling to give alternating copolymers, poly(diindenothiophene-*alt*-bis-[4-(dioctylamino)-phenyl]quinoxaline) **PDIDTDOAQX**, poly-(fluorene-*alt*-bis-[4-(dioctylamino)-phenyl]quinoxaline) **PFDOAQX**, poly(diindenothiophene-*alt*-bis-[4-(dioctylamino)phenyl]thieno-[3,4-*b*]pyrazine) **PDIDTDOATP** and poly(fluorene-*alt*-bis-[4-(dioctylamino)-phenyl]thieno[3,4-*b*]pyrazine) **PFDOATP**, respectively (Scheme 2). All the intermediates, monomers and corresponding copolymers were fully characterized by NMR spectroscopy. The copolymers purified by successive reprecipitation and Soxhlet extraction have narrow molecular weight distributions with a polydispersity index (PDI) below two (Table 1). All of the resulting copolymers show excellent solubility in common organic solvents, such as THF, chloroform, toluene and 1,2-dichlorobenzene.

Thermal properties

PDIDTDOAQX, **PFDOAQX**, **PDIDTDOATP** and **PFDOATP** were analyzed by thermal gravimetric analysis (TGA) and the results are summarized in Table 1. The decomposition temperatures (T_d) of the polymers are situated between 402 and 433 °C

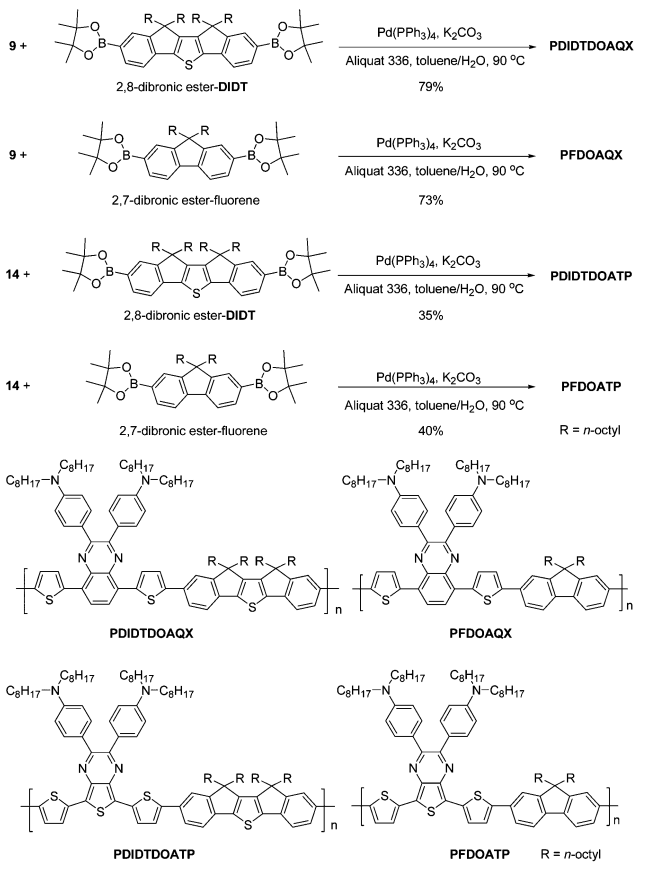

Scheme 2 Synthesis of **PDIDTDOAQX**, **PFDOAQX**, **PDIDIDOATP**, and **PFDOATP**.

Table 1 Molecular weights, polydispersity and thermal properties of polymers

Copolymer	M_w[a]	M_n[a]	PDI[a]	T_d[b] (°C)
PDIDTDOAQX	78 000	39 000	2.00	433
PFDOAQX	27 000	22 000	1.23	432
PDIDTDOATP	14 000	12 000	1.17	409
PFDOATP	14 000	12 000	1.17	402

[a] Molecular weights were determined by gel permeation chromatography (GPC) in THF using polystyrene as the standard. [b] Onset decomposition temperature (5% weight loss) measured by TGA.

(Fig. 3), indicating their sufficient thermal stability for polymer-solar-cell (PSC) applications.

Optical properties

Initially, the absorption spectra of the monomer **DOATP** and an analogue without additional *N*,*N*-dialkylaniline groups on thieno[3,4-*b*]pyrazine, **DEHTP** (Chart 1) are compared in Fig. 4 in order to investigate the influence of the extra donating groups. **DOATP** possesses much stronger absorption in the region from 375 to 475 nm than **DEHTP**. This extra absorption band facilitates photon harvesting in the visible-light region, which is in resonance with our supposition that flanking donating groups can induce additional ICT while photo-excited. The absorption spectra of all studied polymers are illustrated in Fig. 5 (in toluene solution) and Fig. 6 (in thin film), and the corresponding optical parameters are summarized in Table 2. The thin-film spectra do not show significant difference to those in toluene solution except that bathochromic shifts and band-broadening behaviors of the absorption bands were observed in the solid state, suggesting that all polymers in the solid state have stronger intermolecular interactions. All the polymers exhibit two distinct absorption bands. Detailed assignment of the absorption bands with the help of DFT calculations is described in the ESI.† The optical band gaps (E_g^{opt}) estimated from the absorption edges of thin film spectra follow the order: **PFDOAQX** (2.03 eV) > **PDIDTDOAQX** (1.97 eV) > **PFDOATP** (1.62 eV) > **PDIDTDOATP** (1.57 eV). By comparison of these data, it could be deduced that the accepting ability of **DOATP** is stronger than that of **DOAQX**.

With the purpose of further examining the optical effect of the *N*,*N*-dioctylaniline groups on the polymer chains, the interaction between **PDIDTDOATP** and $B(C_6F_5)_3$ was investigated. Given that $B(C_6F_5)_3$ binds to the Lewis basic nitrogen atoms on the *N*,*N*-dioctylaniline moieties, it will result in a

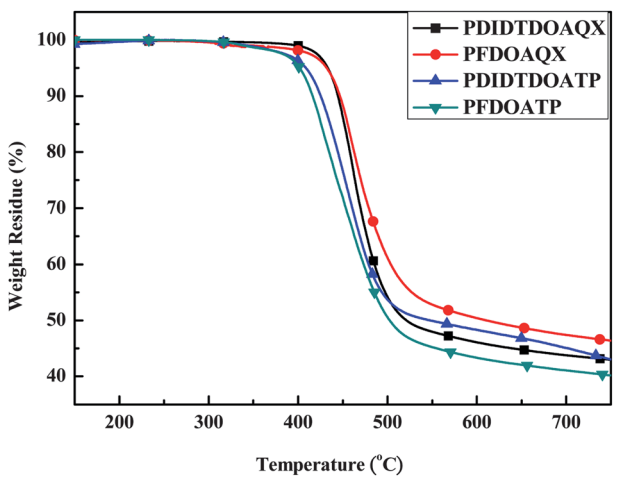

Fig. 3 Thermal gravimetric analysis (TGA) measurements of **PDIDTDOAQX**, **PFDOAQX**, **PDIDTDOATP** and **PFDOATP** with a ramping rate of 10 °C min^{-1}.

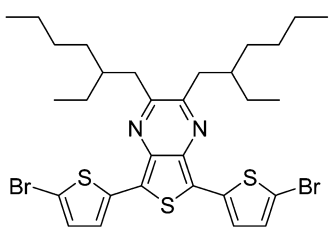

DEHTP

Chart 1 Structure of **DEHTP**.

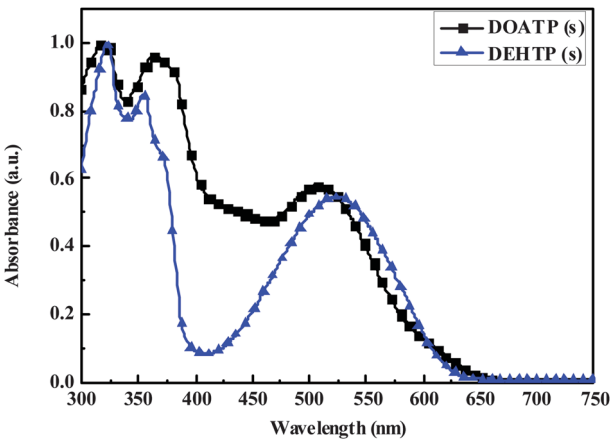

Fig. 4 Normalized absorption spectra of **DOATP** and **DEHTP** in the toluene solution.

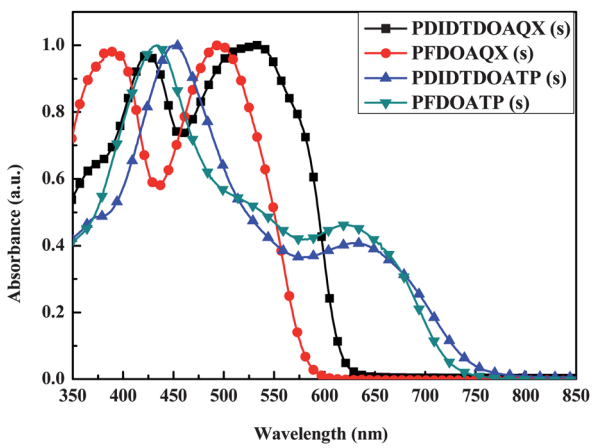

Fig. 5 Normalized absorption spectra of **PDIDTDOAQX**, **PFDOAQX**, **PDIDTDOATP** and **PFDOATP** in toluene solution (0.1 mg per 4 mL).

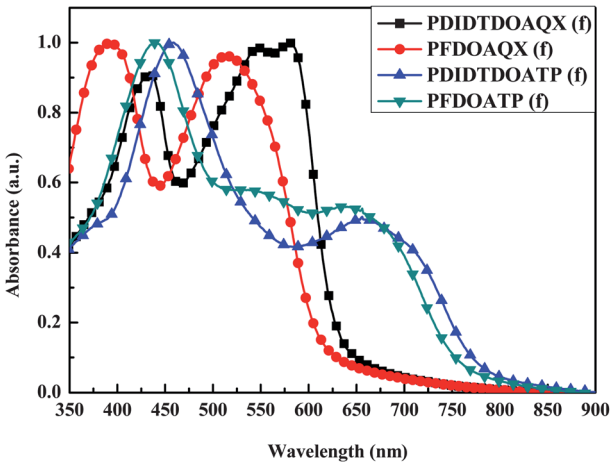

Fig. 6 Normalized absorption spectra of **PDIDTDOAQX**, **PFDOAQX**, **PDIDTDOATP** and **PFDOATP** in thin film.

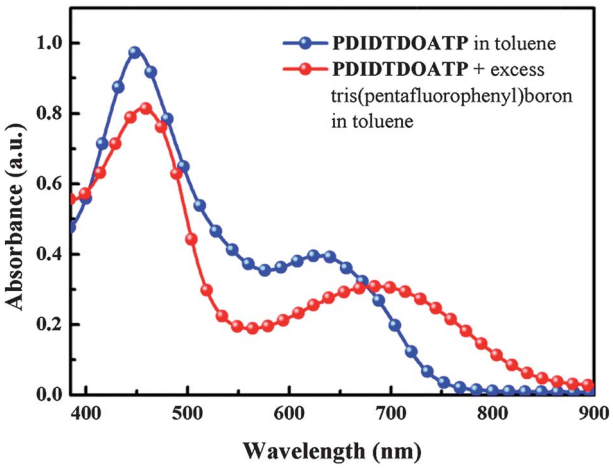

Fig. 7 Normalized absorption spectra of **PDIDTDOATP** (0.064 mg) in toluene (4 mL) solution with and without excess amounts of $B(C_6F_5)_3$ (4 mg).

Table 2 Optical properties and band gaps of the model compounds and copolymers in toluene solution and in thin film[a]

	Toluene solution			Thin film		
Polymer	λ_{max} (nm)	λ_{onset} (nm)	E_g^{opt} (eV)	λ_{max} (nm)	λ_{onset} (nm)	E_g^{opt} (eV)
DOATP	507 364 320	638	1.94			
DEHTP	525 354 322	619	2.00			
PDIDTDOAQX	425, 533	614	2.02	434, 580	629	1.97
PFDOAQX	389, 494	580	2.14	392, 514	611	2.03
PDIDTDOATP	452, 632	747	1.66	464, 656	790	1.57
PFDOATP	433, 632	726	1.71	441, 640	765	1.62

[a] E_g^{opt} was estimated from the onset of UV absorption.

diminution in the ICT band induced by the *N*,*N*-dioctylaniline units and bathochromic shifts of certain absorption bands.[8] Based on the calculation results illustrated in Fig. S1,† the ICT absorptions resulted from the *N*,*N*-dioctylaniline groups are primarily located in the valley from 500–600 nm. As illustrated in Fig. 7, subsequent to the addition of $B(C_6F_5)_3$ to the toluene solution of **PDIDTDOATP**, the absorption intensity of this valley decreased significantly, indicating that the nitrogen atoms on the *N*,*N*-dioctylaniline moieties coordinate to $B(C_6F_5)_3$. The thienopyrazine unit is considered to be less nucleophilic and sterically shielded in **PDIDTDOATP**. Therefore, complexation of the thienopyrazine unit with $B(C_6F_5)_3$ is less likely. Coordination to $B(C_6F_5)_3$ should also make the thienopyrazine moiety more electron-deficient, resulting in the enhancement of the ICT intensity, which is not the case in our observation.

Furthermore, an obvious bathochromic shift was observed for the absorption peak at 632 nm which is mainly the ICT from **DIDT** to thienopyrazine. Since the complexation of $B(C_6F_5)_3$ with the *N*,*N*-dioctylaniline units would make the thienopyrazine group more electron-deficient, the energy band gap of the ICT band from **DIDT** to thienopyrazine is thus lowered, resulting in the evident bathochromic shift.

Electrochemical properties

Cyclic voltammetry (CV) was employed to examine the electrochemical properties and evaluate the HOMO and LUMO energy levels of the polymers. The spectra are illustrated in Fig. 8 and the results are summarized in Table 3. All polymers reveal stable and reversible p-doping and n-doping processes that are important prerequisites for p-type semiconductor materials. The LUMO energy levels of **PDIDTDOAQX**, **PFDOAQX**, **PDIDTDOATP**, and **PFDOATP** are determined to be −3.29, −3.27, −3.61, −3.59 eV, respectively. It is evident that with the same

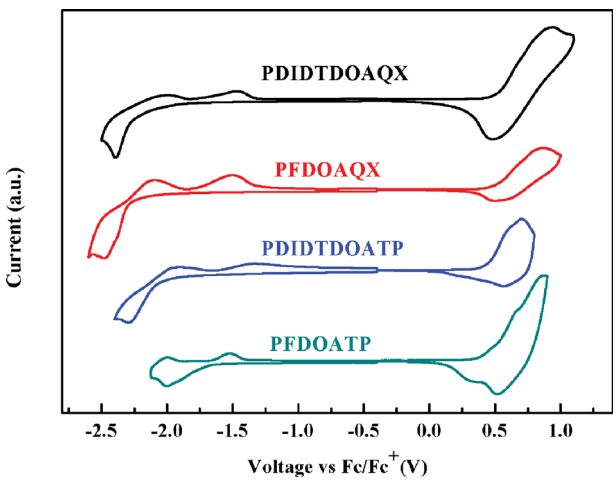

Fig. 8 Cyclic voltammograms of **PDIDTDOAQX**, **PFDOAQX**, **PDIDTDOATP** and **PFDOATP** in thin films at a scan rate of 80 mV s^{-1}.

Table 3 Electrochemical onset potentials and electronic energy levels of the polymers

Copolymer	E_{ox}^{onset} (V)	E_{red}^{onset} (V)	HOMO (eV)	LUMO^{el} (eV)	LUMO^{opt}[a] (eV)	E_g^{el} (eV)
PDIDTDOAQX	0.46	−1.85	−5.26	−2.95	−3.29	2.31
PFDOAQX	0.50	−1.90	−5.30	−2.90	−3.27	2.40
PDIDTDOATP	0.38	−1.65	−5.18	−3.15	−3.61	2.03
PFDOATP	0.41	−1.73	−5.21	−3.07	−3.59	2.14

[a] LUMO^{opt} = HOMO + E_g^{opt}.

acceptor, either **DOAQX** or **DOATP**, the LUMO energy levels of the conjugated polymers do not vary appreciably with variation of the donor unit, indicating that the LUMO energy level is primarily decided by the acceptor. Furthermore, all LUMO energy levels are higher than that of the n-type material, $PC_{71}BM$ (−3.8 eV), ensuring energetically favorable electron transfer. The HOMO energy levels of **PDIDTDOAQX**, **PDIDTDOATP**, **PFDOAQX**, and **PFDOATP** are estimated to be −5.26, −5.18, −5.30, and −5.21 eV. With the same donor (**DIDT** or **F**), the energy level of the HOMO of the polymers rises considerably when the acceptor unit changes from **DOAQX** to **DOATP**, suggesting that the electron density of the HOMO for the studied polymers is not only localized on the donor unit but also distributed elsewhere. An energy diagram of HOMO and LUMO levels of **PDIDTDOAQX**, **PFDOAQX**, **PDIDTDOATP** and **PFDOATP** relative to $PC_{71}BM$ is shown in Fig. 9.

Theoretical calculations

The absorption optical characteristics of the conjugated molecules were investigated at the B3LYP/6-311G(d,P)//TD-B3LYP/6-311G(d,p) level of theory by applying the polarized continuum model (PCM). The computational details are described in the ESI.† Considering an insignificant effect on electronic properties, all the aliphatic substituents were replaced with methyl groups for simplicity. Repeating units, denoted as **DIDTDOAQX**, **FDOAQX**, **DIDTDOATP**, and **FDOATP**, in their most stable conformations were used as simplified model compounds for **PDIDTDOAQX**, **PFDOAQX**, **PDIDTDOATP**, and **PFDOATP**, respectively. The calculated HOMO/LUMO energy, excitation energy, oscillator strength, and configurations of the excited states are summarized in Table 4 and the frontier orbitals, HOMO (H) and LUMO (L) are illustrated in Fig. 10. Although there are variations in the absolute values, the calculated absorptions are still in good agreement with the experimental values. First of all, by comparison of the electronic transitions of **DOATP** and **DEHTP**, it shows that **DOATP** possesses noticeable absorptions between 629 and 378 nm, which are yet absent in **DEHTP**. Analogous phenomena are observed as well in the experimental absorption spectra, albeit the variations in the absolute values exist. In order to have further understanding of these electronic transitions, electron density difference maps (EDDMs) were conducted.[9] The electronic transitions can therefore be visualized through EDDMs. Red indicates a decrease in charge density, while green indicates an increase. For **DEHTP**, the two major transitions (λ_{calc} = 597 and 362 nm) are illustrated in Fig. 11, which reveals that both absorptions mainly derive from the ICT from the thiophene moieties to the pyrazine unit. Furthermore, the electron redistributions of **DEHTP** at 597 and 362 nm are similar to those of **DOATP** at 629 and 378 nm, where the contribution of the flanking *N*,*N*-dimethylaniline groups is insignificant (Fig. 11). In contrast, the additional absorption bands at 584 and 500 nm in **DOATP**

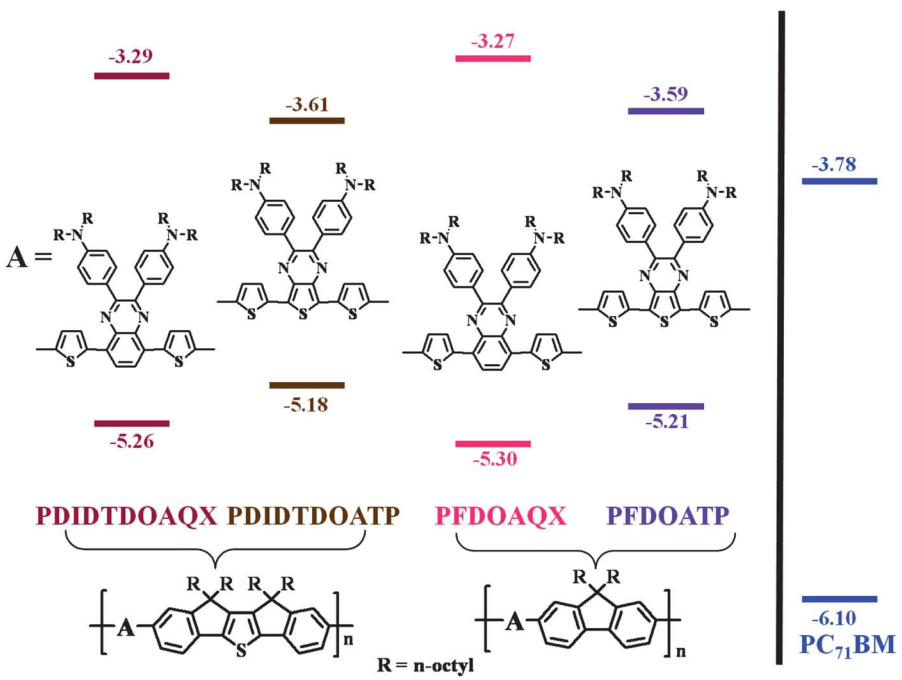

Fig. 9 Energy diagram of HOMO–LUMO levels for **PDIDTDOAQX**, **PFDOAQX**, **PDIDTDOATP**, **PFDOATP** and $PC_{71}BM$.

Table 4 Calculated[a] HOMO/LUMO energy, excitation energy, oscillator strength, and configuration (with large CI coefficients) of the excited state

Compound	HOMO [ev]	LUMO [ev]	Excitation energy $\lambda_{max,exp}$[b] [nm]	Excitation energy λ_{calc} [nm]	Oscillator strength	Symmetry	Configuration[c]
DEHTP	−5.29	−2.86		597	0.5155	Singlet-A	**H→L**
				362	0.6186	Singlet-A	**H→L+1**
DOATP	−5.02	−2.71		629	0.2715	Singlet-A	**H→L**
				584	0.4007	Singlet-A	**H−1→L**
				500	0.2212	Singlet-A	**H−2→L**
				378	0.1884	Singlet-A	H−3→L
							H→L+1
							H−6→L
				373	0.6874	Singlet-A	**H→L+2**
DIDTDOAQX	−4.96	−2.30	533	551	0.875	Singlet-A	**H→L**
							H−1→L
				514	0.3267	Singlet-A	H→L
							H−1→L
				456	0.0877	Singlet-A	**H−2→L**
							H−3→L
			425	427	0.9777	Singlet-A	H−3→L
							H→L+1
FDOAQX	−5.09	−2.29	494	527	0.4946	Singlet-A	**H→L**
							H−1→L
				508	0.406	Singlet-A	H→L
							H−1→L
				448	0.1914	Singlet-A	**H−2→L**
			389	386	0.5775	Singlet-A	**H→L+1**
							H−3→L
							H−1→L+1
DIDTDOATP	−4.75	−2.59	632	684	0.7262	Singlet-A	**H→L**
				570	0.3551	Singlet-A	**H−1→L**
				508	0.1155	Singlet-A	H−3→L
							H−2→L
			452	466	0.9754	Singlet-A	**H→L+1**
							H−2→L
FDOATP	−4.81	−2.59	632	662	0.5282	Singlet-A	**H→L**
				569	0.3659	Singlet-A	**H−1→L**
				493	0.1781	Singlet-A	**H−2→L**
			433	433	0.6958	Singlet-A	**H→L+1**
							H−3→L

[a] TD-B3LYP/6-311G(d,p), PCM = toluene. [b] Experimental values were measured for non-simplified compounds in the toluene solution. [c] Configurations with largest coefficients in the CI expansion of each state are highlighted in boldface.

primarily result from the intramolecular charge transfer from the *N*,*N*-dimethylaniline groups to the **TP** unit. The calculation results strongly suggest that flanking donating groups can induce additional ICT absorptions when photo-excited and validate that our strategy of employing the flanking donating groups to build the D–A(D) two-dimensional conjugated polymer is an effective approach to enhance the absorption ability of the PSC devices.

For the polyaromatic π-electron systems, consistent with the electrochemical experiments, the calculated HOMO energy levels of the four model compounds follow the order: **FDOAQX** (−5.09 eV) < **DIDTDOAQX** (−4.96 eV) < **FDOATP** (−4.81 eV) < **DIDTDOATP** (−4.75 eV) and the calculated LUMO energy levels are in the following sequence: **DIDTDOATP** (−2.59 eV) ≈ **FDOATP** (−2.59 eV) < **DIDTDOAQX** (−2.30 eV) < **FDOAQX** (−2.29 eV). Furthermore, as demonstrated in Fig. 10, for all model compounds, the LUMO electron density is mainly located on the acceptors (**DOAQX** and **DOATP**), supporting the deduction obtained from the electrochemical measurements that the LUMO energy level is primarily decided by the acceptor. The HOMO electron density is not only distributed on the donor but also elsewhere, which is also in resonance with the experimental results. The EDDMs of the polymers are depicted in the ESI.†

Hole-mobility and photovoltaic characteristics

Bulk heterojunction PSCs were fabricated on the basis of ITO/PEDOT:PSS/polymer:$PC_{71}BM$/Ca/Al configuration and their performances were measured under 100 mW cm^{-2} AM1.5 illumination. Hole-only devices (ITO/PEDOT:PSS/polymer/Au) were also fabricated in order to estimate the hole mobilities of these polymers by means of the space-charge limit current (SCLC) theory. The photovoltaic characteristics are summarized in Table 5 and the *J*–*V* curves of these polymers are shown in Fig. 12. The hole mobilities of the polymers are in the following

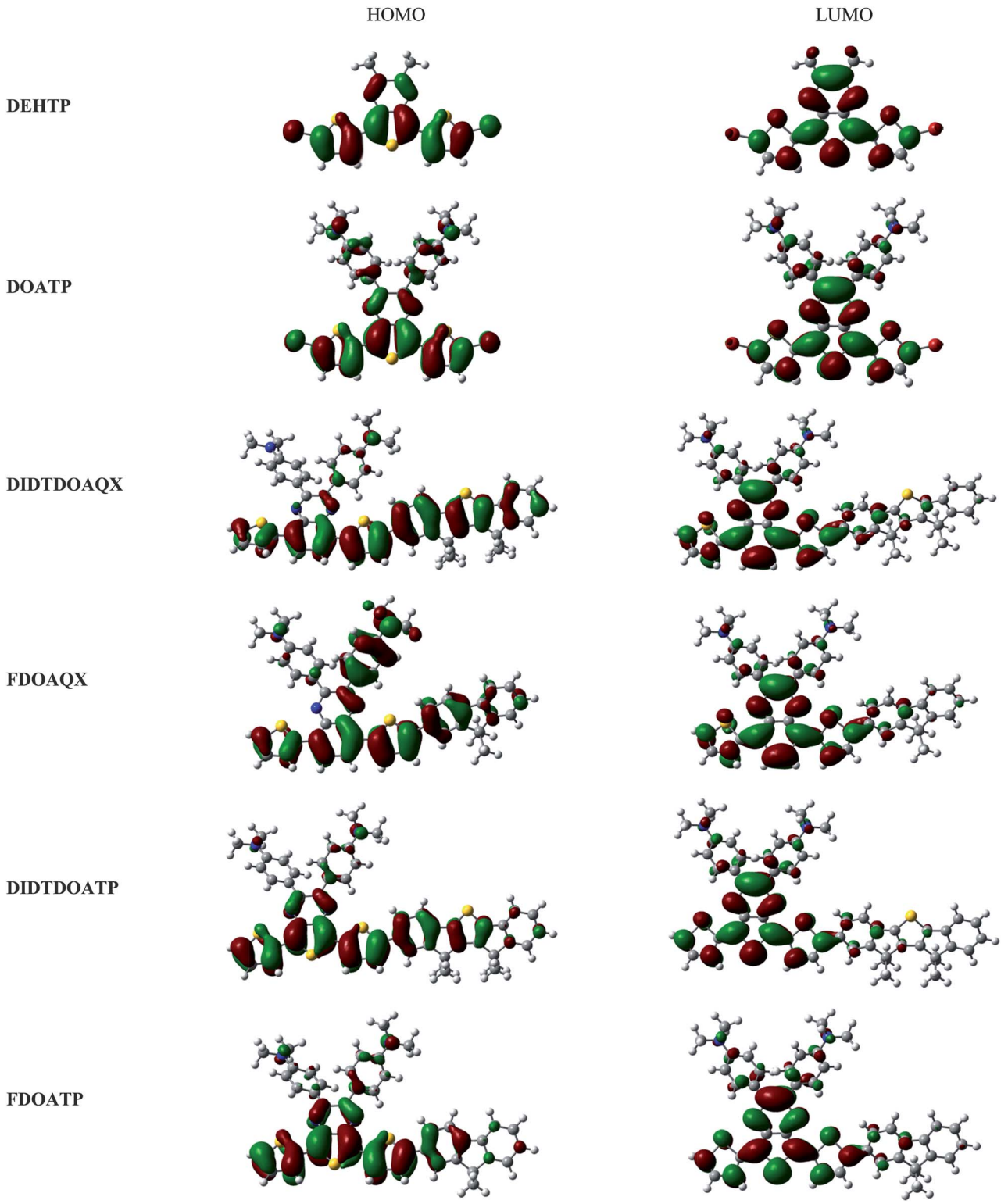

Fig. 10 Plots (isovalue = 0.02 au) of frontier orbitals of **DEHTP**, **DOATP**, **DIDTDOAQX**, **FDOAQX**, **DIDTDOATP**, and **FDOATP**, calculated at the level of B3LYP/6-311G(d,P) in THF.

order: **PFDOATP** (3×10^{-6} cm^2 V^{-1} s^{-1}) ≈ **PDIDTDOATP** (3×10^{-6} cm^2 V^{-1} s^{-1}) < **PFDOAQX** (1×10^{-5} cm^2 V^{-1} s^{-1}) < **PDIDTDOAQX** (5×10^{-5} cm^2 V^{-1} s^{-1}), suggesting that the **DOAQX**-based polymers have higher hole mobility than the **DOATP**-based polymers. The device based on **PDIDTDOAQX**/$PC_{71}BM$ and **PFDOAQX**/$PC_{71}BM$ showed PCEs of 1.94 and 1.65%, respectively, which are higher than the analogous devices based on **PFDOATP**/$PC_{71}BM$ (PCE = 0.5%) and

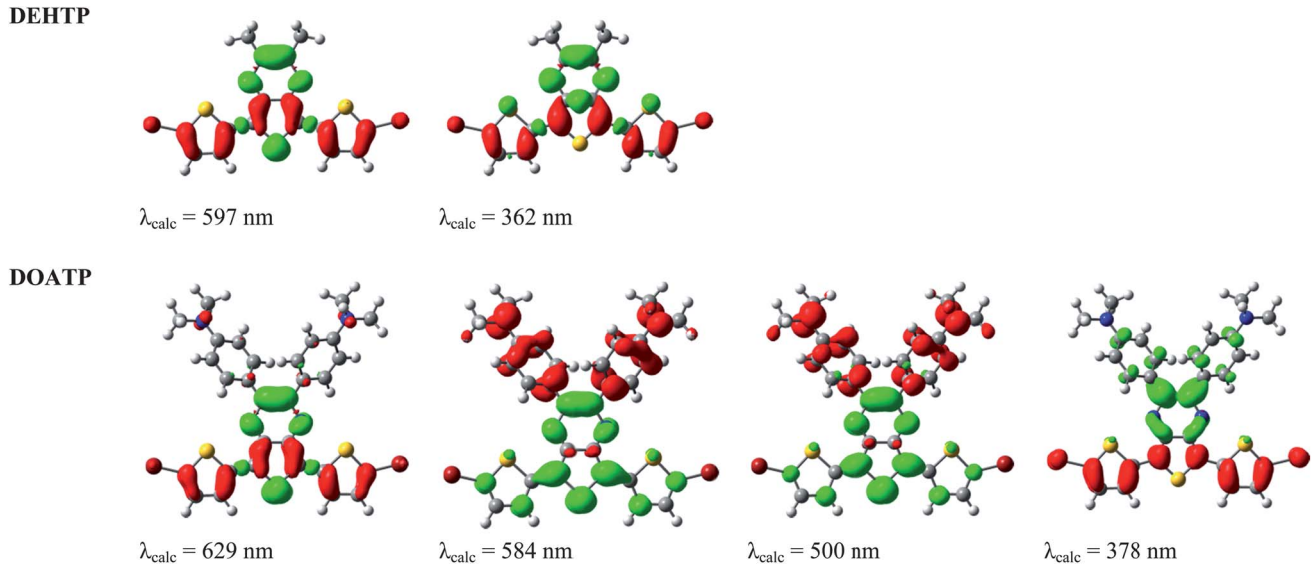

Fig. 11 Electron density difference maps (EDDMs) of selected singlet electronic transitions of **DEHTP** (at 597 and 362 nm) and **DOATP** (at 629, 584, 500, and 378 nm). Red indicates a decrease in charge density, while green indicates an increase. All EDDMs are plotted with isovalue 0.0012 au.

Table 5 Photovoltaic characteristics

Copolymer	Polymer:$PC_{71}BM$ (wt %)	Mobility ($cm^2\ V^{-1}\ s^{-1}$)	V_{oc} (V)	J_{sc} ($mA\ cm^{-2}$)	FF (%)	PCE (%)
PDIDTDOAQX	1 : 1	5×10^{-5}	0.62	−6.79	46	1.94
PFDOAQX	1 : 1	1×10^{-5}	0.72	−5.52	41	1.65
PDIDTDOATP	1 : 1	3×10^{-6}	0.60	−3.11	41	0.77
PFDOATP	1 : 1	3×10^{-6}	0.68	−2.25	32	0.50

PDIDTDOATP/$PC_{71}BM$ (PCE = 0.77%). The performances of these solar devices are in good agreement with their J_{sc} values, which are highly associated with the hole mobilities of the polymers. Besides, the molecular weight of polymers may also affect the device efficiency. **PDIDTDOAQX** with the highest molecular weight among the four polymers has the highest PCE. It is likely that longer polymer chains could enhance the hole mobility of polymers and provide more contact between polymers and fullerenes, leading to higher device performances.

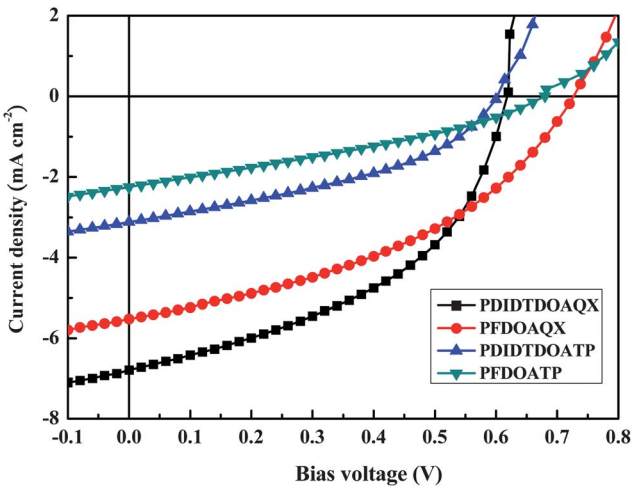

Fig. 12 *J–V* characteristics of ITO/PEDOT:PSS/polymer:$PC_{71}BM$/Ca/Al under illumination of AM1.5, 100 mW cm^{-2}.

Conclusions

We have successfully designed and synthesized a series of novel two-dimensional conjugated copolymers with the D_1–A(D_2) repeating pattern. This construction strategy can result in at least two strong ICT absorptions and therefore superior light harvesting, which was evaluated experimentally by absorption spectroscopy and computationally by DFT calculations. The photovoltaic performances of the devices incorporating these polymers follow the sequence: **PDIDTDOAQX** > **PFDOAQX** > **PDIDTDOATP** > **PFDOATP**, which is in good agreement with the trend of their hole-mobilities. The device based on **PDIDTDOAQX**/$PC_{71}BM$ exhibited the highest J_{sc} of 6.79 mA cm^{-2} and a PCE of 1.94%.

Notes and references

1 (*a*) G. Yu, J. Gao, J. C. Hummelen, F. Wudl and A. J. Heeger, *Science*, 1995, **270**, 1789–1791; (*b*) B. C. Thompson and

J. M. J. Fréchet, *Angew. Chem., Int. Ed.*, 2008, **47**, 58–77; (*c*) S. Günes, H. Neugebauer and N. S. Sariciftci, *Chem. Rev.*, 2007, **107**, 1324–1388; (*d*) Y.-J. Cheng, S.-H. Yang and C.-S. Hsu, *Chem. Rev.*, 2009, **109**, 5868–5923; (*e*) J. Chen and Y. Cao, *Acc. Chem. Res.*, 2009, **42**, 1709–1718; (*f*) H. Zhou, L. Yang and W. You, *Macromolecules*, 2012, **45**, 607–632.

2 (*a*) W. J. E. Beek, M. M. Wienk, M. Kemerink, X. Yang and R. A. J. Janssen, *J. Phys. Chem. B*, 2005, **109**, 9505–9516; (*b*) S. Günes, H. Neugebauer and N. S. Sariciftci, *Chem. Rev.*, 2007, **107**, 1324–1338; (*c*) G. Li, V. Shrotriya, Y. Yao, J. Huang and Y. Yang, *J. Mater. Chem.*, 2007, **17**, 3126–3140; (*d*) M. T. Dang, L. Hirsch and G. Wantz, *Adv. Mater.*, 2011, **23**, 3597–3602.

3 (*a*) J.-S. Wu, Y.-J. Cheng, T.-Y. Lin, C.-Y. Chang, P.-I. Shih and C.-S. Hsu, *Adv. Funct. Mater.*, 2012, **22**, 1711–1722; (*b*) Y.-J. Cheng, C.-H. Chen, Y.-S. Lin, C.-Y. Chang and C.-S. Hsu, *Chem. Mater.*, 2011, **23**, 5068–5075; (*c*) C.-H. Chen, Y.-J. Cheng, M. Dubosc, C.-H. Hsieh, C.-C. Chu and C.-S. Hsu, *Chem.–Asian J.*, 2010, **5**, 2483–2492; (*d*) E. Bundgaard and F. C. Krebs, *Sol. Energy Mater. Sol. Cells*, 2007, **91**, 954–985; (*e*) M. Svensson, F. Zhang, S. C. Veenstra, W. J. H. Verhees, J. C. Hummelen, J. M. Kroon, O. Inganäs and M. R. Andersson, *Adv. Mater.*, 2003, **15**, 988–991; (*f*) C.-A. Tseng, J.-S. Wu, T.-Y. Lin, W.-S. Kao, C.-E. Wu, S.-L. Hsu, Y.-Y. Liao, C.-S. Hsu, H.-Y. Huang, Y.-Z. Hsieh and Y.-J. Cheng, *Chem.–Asian J.*, 2012, **7**, 2102–2110; (*g*) Y.-J. Cheng, S.-W. Cheng, C.-Y. Chang, W.-S. Kao, M.-H. Liao and C.-S. Hsu, *Chem. Commun.*, 2012, **48**, 3203–3205; (*h*) Y. J. Cheng, C.-H. Chen, T.-Y. Lin and C.-S. Hsu, *Chem.–Asian J.*, 2012, **7**, 818–825; (*i*) Y.-L. Chen, C.-Y. Chang, Y.-J. Cheng and C.-S. Hsu, *Chem. Mater.*, 2012, **24**, 3964–3971; (*j*) H.-H. Chang, C.-E. Tsai, Y.-Y. Lai, D.-Y. Chiou, S.-L. Hsu, C.-S. Hsu and Y.-J. Cheng, *Macromolecules*, 2012, **45**, 9282–9291; (*k*) Y.-J. Cheng, Y.-J. Ho, C.-H. Chen, W.-S. Kao, C.-E. Wu, S.-L. Hsu and C.-S. Hsu, *Macromolecules*, 2012, **45**, 2690–2698; (*l*) Y.-X. Xu, C.-C. Chueh, H.-L. Yip, F.-Z. Ding, Y.-X. Li, C.-Z. Li, X. Li, W.-C. Chen and A. K.-Y. Jen, *Adv. Mater.*, 2012, **24**, 6356–6361; (*m*) A. T. Yiu, P. M. Beaujuge, O. P. Lee, C. H. Woo, M. F. Toney and J. M. J. Fréchet, *J. Am. Chem. Soc.*, 2012, **134**, 2180–2185.

4 (*a*) C.-H. Chen, C.-H. Hsieh, M. Dubosc, Y.-J. Cheng and C.-S. Hsu, *Macromolecules*, 2010, **43**, 697–708; (*b*) C.-H. Chen, Y.-J. Cheng, C.-Y. Chang and C.-S. Hsu, *Macromolecules*, 2011, **44**, 8415–8424; (*c*) M. Sommer, S. Huettner and M. Thelakkat, *J. Mater. Chem.*, 2010, **20**, 10788–10797; (*d*) P. P. Khlyabich, B. Burkhart, C. F. Ng and B. C. Thompson, *Macromolecules*, 2011, **44**, 5079–5084; (*e*) B. Burkhart, P. P. Khlyabich, T. C. Canak, T. W. LaJoie and B. C. Thompson, *Macromolecules*, 2011, **44**, 1242–1246; (*f*) J. Li, K.-H. Ong, S.-L. Lim, G.-M. Ng, H.-S. Tan and Z.-K. Chen, *Chem. Commun.*, 2011, **47**, 9480–9482.

5 (*a*) Z.-G. Zhang, S. Zhang, J. Min, C. Chui, J. Zhang, M. Zhang and Y. Li, *Macromolecules*, 2012, **45**, 113–118; (*b*) Z.-G. Zhang, S. Zhang, J. Min, C. Cui, H. Geng, Z. Shuai and Y. Li, *Macromolecules*, 2012, **45**, 2312–2320; (*c*) Y. Li, *Acc. Chem. Res.*, 2012, **45**, 723–733; (*d*) Y. Li and Y. Zou, *Adv. Mater.*, 2008, **20**, 2952–2958; (*e*) J. Hou, Z. Tan, Y. Yan, Y. He, C. Yang and Y. Li, *J. Am. Chem. Soc.*, 2006, **128**, 4911–4916; (*f*) J. Hou, L. Huo, C. He, C. Yang and Y. Li, *Macromolecules*, 2006, **39**, 594–603; (*g*) J. Hou, C. Yang, C. He and Y. Li, *Chem. Commun.*, 2006, 871–873.

6 (*a*) F. Huang, K.-S. Chen, H.-L. Yip, S. K. Hau, O. Acton, Y. Zhang, J. Luo and A. K.-Y. Jen, *J. Am. Chem. Soc.*, 2009, **131**, 13886–13887; (*b*) C. Duan, K.-S. Chen, F. Huang, H.-L. Yip, S. Liu, J. Zhang, A. K.-Y. Jen and Y. Cao, *Chem. Mater.*, 2010, **22**, 6444–6452; (*c*) C. Duan, W. Cai, F. Huang, J. Zhang, M. Wang, T. Yang, C. Zhong, X. Gong and Y. Cao, *Macromolecules*, 2010, **43**, 5262–5268; (*d*) Y.-J. Cheng, L.-C. Hung, F.-Y. Cao, W.-S. Kao, C.-Y. Chang and C.-S. Hsu, *J. Polym. Sci., Part A: Polym. Chem.*, 2011, **49**, 1791–1801; (*e*) Z.-G. Zhang, Y.-L. Liu, Y. Yang, K. Hou, B. Peng, G. Zhao, M. Zhang, X. Guo, E.-T. Kang and Y. Li, *Macromolecules*, 2010, **43**, 9376–9383; (*f*) C. Duan, F. Huang and Y. Cao, *J. Mater. Chem.*, 2012, **22**, 10416–10434.

7 (*a*) P. Baierweck, U. Simmross and K. Müllen, *Chem. Ber.*, 1988, **121**, 2195–2200; (*b*) J. Roncali and C. Thobie-Gautier, *Adv. Mater.*, 1994, **6**, 846–848; (*c*) T. Kowada, T. Kuwabara and K. Ohe, *J. Org. Chem.*, 2010, **75**, 906–913.

8 G. C. Welch and G. C. Bazan, *J. Am. Chem. Soc.*, 2011, **133**, 4632–4644.

9 N. M. O'Boyle, A. L. Tenderholt and K. M. Langner, *J. Comput. Chem.*, 2008, **29**, 839–845.

